



## Proton-air inelastic cross section measurement with ARGO-YBJ

I. DE MITRI<sup>1,4</sup>, D. MARTELLO<sup>1,4</sup>, L. PERRONE<sup>2,4</sup>, A. SURDO<sup>4</sup>, M. ZHA<sup>3</sup>

ON BEHALF OF THE ARGO-YBJ COLLABORATION

<sup>1</sup>*Dipartimento di Fisica, Università del Salento, Lecce, Italy*

<sup>2</sup>*Dipartimento di Ingegneria dell'Innovazione, Università del Salento, Lecce, Italy*

<sup>3</sup>*IHEP (Institute for High Energy Physics), Beijing, China*

<sup>4</sup>*INFN (Istituto Nazionale di Fisica Nucleare), Sezione di Lecce*

*ivan.demitri@le.infn.it*

**Abstract:** First results of the measurement of the interaction cross section between primary protons and air nuclei with the ARGO-YBJ experiment are reported. The analysis is based on the flux attenuation for different atmospheric depths (i.e. zenith angles) and can exploit the detector capabilities of selecting the shower development stage by means of the size, hit density and both time and lateral profile measurements. The effects of shower fluctuations and the contribution of heavier primaries have been also considered.

## Introduction

Cosmic ray physics in the  $10^{12} - 10^{15}$  eV energy range is one of the main scientific goals of the ARGO-YBJ experiment, a full coverage extensive air shower array resulting from a collaboration between Chinese and Italian institutions [1]. The laboratory is located in the village of Yangbajing, near Lhasa, in the Tibet region (People's Republic of China) at an altitude of 4300 m above sea level, corresponding to a vertical atmospheric depth of  $606 \text{ g/cm}^2$ . The detector, extensively described in [1], is logically divided into 154 units called *clusters* ( $7.64 \times 5.72 \text{ m}^2$ ) each made by 12 Resistive Plate Chambers (RPCs) operated in streamer mode. Each RPC ( $1.26 \times 2.85 \text{ m}^2$ ) is read out by using 10 pads ( $62 \times 56 \text{ cm}^2$ ), which are further divided into 8 strips ( $62 \times 7 \text{ cm}^2$ ) providing a larger particle counting dynamic range [2]. The signals coming from all the strips of a given pad are sent to the same channel of a multihit TDC. The whole system provides a single hit (pad) time resolution at the level of 1 ns, which allows a complete and detailed three-dimensional reconstruction of the shower front. Details on all the updated results can be found in the other contributions of the ARGO-YBJ collaboration to this conference [3].

## The cross section measurement

Given a primary energy interval, the frequency of showers as a function of zenith angle  $\theta$ , for a fixed distance  $X_{DM}$  between the detector and the shower maximum, is directly related to the probability distribution of the depth of the shower maximum itself  $P(X_{max})$ , with  $X_{max} = h_0 \sec\theta - X_{DM}$ , where  $h_0$  is the observation vertical depth. The shape of  $P(X_{max})$  is given by the folding of the exponential dependence of the depth of the first interaction point  $X_0$  (i.e.  $e^{-X_0/\lambda_p}$  with  $\lambda_p(\text{g/cm}^2) \simeq 2.41 \cdot 10^4 / \sigma_{p-Air}(\text{mb})$ ), with the probability distribution of  $X_{rise} = X_{max} - X_0$ , which takes into account the fluctuations of the shower development up to its maximum. For sufficiently large  $X_{max}$  values,  $P(X_{max})$  tends to have a simple exponential falling behaviour with an attenuation length  $\Lambda = \kappa \lambda_p$ , where  $\kappa$  depends on the shower development in the atmosphere, on its fluctuations and on the detector response. The value of  $\kappa$  must be evaluated by Monte Carlo (MC) simulations, and it might depend on the features of the adopted hadronic interaction model, even if several studies showed that the dependence is small [4, 5]. Finally, the contribution of cosmic rays heavier than protons have to be estimated, or at least mini-

mized in the analyzed data sample, in order to get an unbiased proton-air cross section estimate.

Experiments using the air fluorescence technique have direct access to  $P(X_{max})$  [6, 7], while EAS detectors measuring the particles at ground might sample it through the flux dependence on the zenith angle. In particular, the number of muons  $N_\mu$  is used to select the energy range and the size  $N_e$  is used to fix  $X_{DM}$  (or the shower age), after having selected a proton enriched sample on the basis of the  $e/\mu$  content [8, 9, 10].

As pointed out in [11, 12], shower fluctuations play a major role and might decrease the experimental sensitivity to  $\sigma_{p-Air}$ . Since these effects depend on cosmic ray energy range and chemical composition, on the detector capabilities and location, and on the actual analysis procedure, the sensitivity of each given experiment/technique has to be checked with detailed simulations. Good performance is obtained if the exponential tail of  $P(X_{max})$  can be studied, otherwise a flattening of the distribution might be observed, mainly due to shower fluctuations, resulting in larger value of the parameter  $\kappa$  and a lower sensitivity to  $\lambda_p$ .

The ARGO-YBJ detector features and location (full coverage, angular resolution, fine granularity, small atmospheric depth, etc.) can be used to fix the energy ranges and to constrain the shower ages. In particular, different hit multiplicity windows can be used to select showers corresponding to different primary energies, while the information on particle density, lateral profile and shower front can constrain  $X_{DM}$  in a range that makes possible the observation of the exponential falling of  $P(X_{max})$  through the  $sec\theta$  distribution (once the geometrical acceptance in each angular bin has been taken into account).

## Data Selection and Analysis results

The analysis started from a data sample of about  $10^7$  events. In order to have both a small contamination of external events (i.e. those with the true core position outside the carpet but reconstructed inside) and an angular resolution better than  $0.5^\circ$  [3], only events with at least 300 fired pads were considered.

After a first selection based on the quality of the reconstruction procedure, a further rejection of external showers (misreconstructed as internal ones) was performed by means of the following cuts. The reconstructed core position,  $P_{rc}$ , was required to be in a fiducial surface given by the inner  $11 \times 8$  RPC clusters [3]. The quantity  $R_{70}$  was then defined as the radius of a circle (centered in  $P_{rc}$ ) containing 70% of the fired strips. It was required that the distance of  $P_{rc}$  from the detector center plus  $R_{70}$  to be less than 50 m. Finally a minimum average fired strip density, within  $R_{70}$ , was set at  $0.2/m^2$  (in the shower plane).

A full simulation of the detector response, including the trigger, the reconstruction chain, etc., was performed in order to check the effects of the different analysis cuts. About  $7 \cdot 10^5$  proton initiated showers, with the proper power law energy spectrum between 100 GeV and 1000 TeV and zenith angle up to  $45^\circ$ , were produced with Corsika [13] using QGSJET as interaction model [14].

The data sample was split into two different bins of fired pads  $N_{pad}$ , namely  $300 \leq N_{pad} \leq 1000$  and  $N_{pad} > 1000$ , corresponding to different energy intervals with average values of  $E^{(1)} = (3.9 \pm 0.1)$  TeV and  $E^{(2)} = (12.7 \pm 0.4)$  TeV respectively (estimated after all the analysis cuts). Simulations have also shown that, after the analysis cuts, the contamination of external events amounts to 20% and 0.4% for the two energy bins respectively.

Several studies were performed in order to find proper observable quantities suitably correlated with the detector distance from the first interaction point,  $X_{D0}$ , or from the shower maximum,  $X_{DM}$ . A correlation between  $X_{D0}$  and  $R_{70}$  has been found, which allows selecting events that interacted deeper in the atmosphere, by using the aforementioned cuts and by requiring  $R_{70}$  to be sufficiently small. In our case  $R_{70} < 25$  m has been found to give good results.

A check was made that the event selection, both in primary energy and shower age (or  $X_{D0}$ ) is independent of the zenith angle up to about  $40^\circ$ , thus showing that the experimental sensitivity is not compromised by shower fluctuations [11, 12].

Further important improvements can be reached by using a more detailed information on the lateral profile and on the shower front (curvature, rise

time, time width, etc.) that ARGO-YBJ is able to record with very high precision [3]. An improved analysis using also these information is in progress.

We have then analyzed a data sample of  $10^5$  events with total pad multiplicity  $N_{pad} > 300$  and zenith angle  $\theta < 40^\circ$ . About 4% of them actually came through all the analysis cuts (the same fraction has been found in the MC). The result of the whole procedure is reported in figure 1 where the experimental  $sec\theta$  distributions for the two pad multiplicity (i.e. energy) ranges are shown, after correcting for the geometrical acceptance of each angular bin. They clearly show the expected exponential behaviour, with a slight deviation at small  $sec\theta$  values (therefore not included in the fit) for the low energy sample only. This is accounted for the larger contamination of external events, even if there might also be a contribution of shower fluctuations, the shower maximum being more distant from the detector (in average  $X_{max} \simeq 390$  g/cm<sup>2</sup> for the low energy sample, while  $X_{max} \simeq 450$  g/cm<sup>2</sup> for the other one).

The  $sec\theta$  distributions obtained from the full simulation show very similar behaviours to the ones obtained with data and the same considerations can be applied. From these plots the values of  $\kappa$  can be extracted by comparing the fitted value of  $\Lambda_{MC}$  with the one,  $\lambda_p$ , assumed in the simulation (i.e. from QGSJET). We obtain  $\kappa_1 = 1.6 \pm 0.3$  and  $\kappa_2 = 1.2 \pm 0.1$  for the low and high energy bin respectively. As can be seen, the  $\kappa_2$  value is completely consistent with previous works [4, 8, 9, 10, 11, 12], while  $\kappa_1$  is slightly larger than expected. This is a direct consequence of the observed flattening of the  $sec\theta$  distribution at low energies (see above).

The measured  $\Lambda_{DATA}$  values together with the  $\kappa$  determined from simulation, directly give the cross section  $\bar{\sigma}_{p-Air}$  (still to be corrected for the heavier primaries) at the two energies. By applying this procedure we get  $\bar{\sigma}_{p-Air}^{(1)} = (299 \pm 55)$  mb and  $\bar{\sigma}_{p-Air}^{(2)} = (306 \pm 34)$  mb, for the low and high energy bin respectively.

An estimate of the systematics introduced by cosmic ray primaries heavier than protons has been performed by evaluating the effect on the shape of the  $sec\theta$  distribution with the introduction of helium primaries in the simulated data. Both the dif-

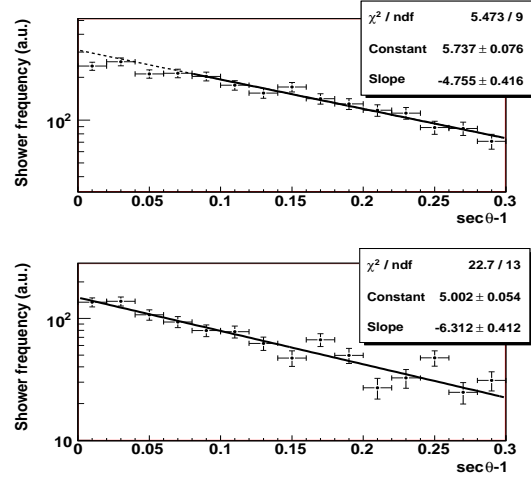


Figure 1: Experimental  $sec\theta$  distributions for the low (above) and high (below) pad multiplicity samples, after the correction for the geometrical acceptance in each angular bin.

ferent absolute values and the energy dependences of proton and helium fluxes were considered. As expected the simulations showed a slight steepening of the  $sec\theta$  distribution, thus changing the values of the estimated cross section. By using different primary flux measurements given in the literature [15, 16, 17] we found correction factors within 7% and 9%. The corrected proton-air cross sections are then given by:

$$\begin{aligned}\sigma_{p-Air}^{(1)} &= (275 \pm 51) \text{ mb} \\ \sigma_{p-Air}^{(2)} &= (282 \pm 31) \text{ mb}\end{aligned}$$

where statistical errors are reported. Corrections for other primaries (i.e. CNO group, Fe, etc.) are expected to be negligible. As shown in figure 2 these results are in agreement with previous measurements and make us even more confident of this method, with increased statistics, for the estimation of  $\sigma_{p-Air}$  at high energies up to the limit of the ARGO-YBJ sensitivity (around 1000 TeV, i.e.  $\sqrt{s} \simeq 1.4$  TeV).

From the  $\sigma_{p-Air}$ , the total proton-nucleon  $\sigma_{p-N}$  cross section can be derived by using different models [5, 18, 19, 20]. The results, for the two energy bins, are:  $\sigma_{p-N}^{(1)} = (40 \pm 7)$  mb and  $\sigma_{p-N}^{(2)} =$

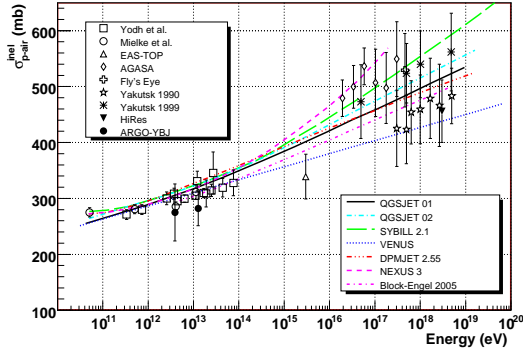


Figure 2: Inelastic  $p - Air$  cross section measured by different experiments. The prediction of several hadronic interaction models are also shown. In this plot ARGO-YBJ data points have already been corrected for the contribution of primaries heavier than protons.

$(43 \pm 5)$  mb, that are in good agreement with the extrapolation of other measurements to the ARGO-YBJ energy region. To these values a further systematic uncertainty must be applied coming from the differences among theoretical models, which in our energy range lie within few percent.

## Discussion and Conclusions

As evidenced by both the shape of the  $sec\theta$  distributions and the value of the factors  $\kappa$ , fluctuations might play a role in the low energy region only, while the high energy sample behaves as unaffected. In fact, the lower energy limit of this first analysis was actually set by the contamination of external events, whose contribution produces a slightly flatter  $sec\theta$  distribution thus giving a value of  $\kappa_1$  larger than the one that can actually be obtained. Studies are in progress in order to reduce the contamination at energies below few TeV.

In conclusions, the results of this work show the reliability of the adopted technique. The measured proton-air cross sections are in agreement with previous works, and estimates of the proton-nucleon cross sections lie on the high energy extrapolation of accelerator data. Further studies are in progress to fully exploit the ARGO-YBJ detector capabili-

ties in selecting the shower development stage and to extend the covered primary energy region up to  $10^3$  TeV, by also using the RPC analog readout [3].

## References

- [1] C. Bacci, et al., *Astropart. Phys.* 17 (2002) 151–165, and references therein.
- [2] G. Aielli, et al., *Nucl. Instrum. Meth.* A562 (2006) 92–96.
- [3] D. Martello, et al., First results from the ARGO-YBJ experiment, in: *Proceedings of the 30<sup>th</sup> International Cosmic Ray Conference, Merida (Mexico), 2007*, and references therein.
- [4] C. L. Pryke, *Astropart. Phys.* 14 (2001) 319–328.
- [5] M. M. Block, *Phys. Rept.* 436 (2006) 71–215, and references therein.
- [6] R. M. Baltrusaitis, et al., *Phys. Rev. Lett.* 52 (1984) 1380–1383.
- [7] K. Belov, *Nucl. Phys. Proc. Suppl.* 151 (2006) 197–204.
- [8] T. Hara, et al., *Phys. Rev. Lett.* 50 (1983) 2058–2061.
- [9] M. Honda, et al., *Phys. Rev. Lett.* 70 (1993) 525–528.
- [10] M. Aglietta, et al., *Nucl. Phys. Proc. Suppl.* 75A (1999) 222–224.
- [11] J. Alvarez-Muniz, et al., *Phys. Rev.* D66 (2002) 123004.
- [12] J. Alvarez-Muniz, et al., *Phys. Rev.* D69 (2004) 103003.
- [13] J. Knapp, D. Heck, *Nachr. Forsch. zentr. Karlsruhe* 30 (1998) 27–37.
- [14] N. N. Kalmykov, et al., *Nucl. Phys. Proc. Suppl.* 52B (1997) 17–28.
- [15] K. Asakimori, et al., *Astrophys. J.* 502 (1998) 278–283.
- [16] A. V. Apanasenko, et al., *Astropart. Phys.* 16 (2001) 13–46.
- [17] J. R. Horandel, *Astropart. Phys.* 19 (2003) 193–220.
- [18] R. J. Glauber, G. Matthiae, *Nucl. Phys.* B21 (1970) 135–157.
- [19] L. Durand, H. Pi, *Phys. Rev.* D38 (1988) 78–84.
- [20] T. Wibig, D. Sobczynska, *J. Phys.* G24 (1998) 2037–2047.